CAERM: Coverage Aware Energy Replenishment Mechanism Using Mobile Charger in Wireless Sensor Networks

Hongli Yu, Chih-Yung Chang, *Member, IEEE*, Yajun Wang, Diptendu Sinha Roy, and Xing Bai

***Abstract*—Wireless charging is one of the most important issues in wireless sensor networks (WSNs), which aims to cope with the energy limitation problem of the sensors. Many of the existing researches applied the mobile charger to recharge the sensors for maintaining the perpetual lifetime of sensor networks. However, when choosing sensors to be recharged, the coverage contribution of sensors was ignored. This paper proposes a recharging scheme, called CAERM, which considers the coverage contribution of each requested sensor and constructs the recharging path to maximize the coverage of the whole networks. Two algorithms, including Simple Recharging Coverage Benefit (S-RCB) and Chain-Effect Recharging Coverage Benefit (CE-RCB) algorithms, are proposed to evaluate the coverage contribution of the requested sensors effectively. Through extensive simulations, experimental study shows that the proposed algorithm improves the recharging efficiency, while maximizing the coverage contribution and monitoring quality of the given sensor networks.**

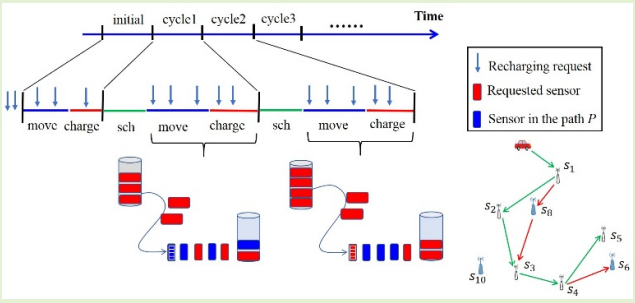

***Index Terms*—Rechargeable sensors, energy recharging, mobile charger, coverage contribution, wireless sensor networks.**

I. Introduction

WIRELESS sensor networks (WSNs) have been widely applied in various applications. In the industry systems, the wireless sensor network was deployed to monitor the working status of the equipment [1], [2]. The wireless sensors were also used to provide sensing services to IoT devices with limited energy and storage resources [3]–[5]. Besides, the WSNs provided smart agriculture with effective solutions for collecting, transmitting, and processing of information [6]. Study [7] proposed the attack detection and isolation mechanism for critical smart grid applications, which significantly enhanced the power efficiency. However, the wireless sensors are mainly powered by batteries with limited energy, leading to the problem of limited network lifetime.

To cope with the problem of limited network lifetime, many schemes have been proposed. Some studies aimed to cope with the energy shortage issue from the perspective of data collection [8]–[10]. While other studies focused on how to decrease the energy consumption of sensors by shortening the length of the data transmission path [11]. However, these methods cannot prevent the death of sensor networks. Recently, the wireless recharging technology [12], [13] has achieved rapid development, which provides an effective solution for the energy supply of wireless sensor networks. These studies can be mainly divided into two categories: static recharging approaches and dynamic recharging approaches.

In the static recharging class [14]–[16], the proposed mechanisms assumed that the mobile charger was aware of the information including energy consumption rate, last recharging time and sensor locations. The mobile recharger was arranged to travels along the fixed path in the monitor scenes to replenish energy for the sensors. In study [17], a mobile charger was used to travel inside the sensor network periodically, with the objective of maximizing the ratio of the mobile charger's vacation time over the cycle time. The core problem to be solved in these mechanisms is how to plan the recharging path for the mobile charger to satisfy the recharging requirement

Manuscript received July 22, 2021; accepted September 6, 2021. Date of publication September 10, 2021; date of current version October 18, 2021. This research is partially sponsored by the National Natural Science Foundation of Liaoning Province (No. 2020-MS-291). The associate editor coordinating the review of this article and approving it for publication was Dr. Thilo Sauter. *(Corresponding author: Chih-Yung Chang.)*

Hongli Yu, Yajun Wang, and Xing Bai are with the School of Electronics and Information Engineering, Liaoning University of Technology, Jinzhou 121001, China (e-mail: hly@chzu.edu.cn; wyj_lg@163.com; b593548023@163.com).

Chih-Yung Chang is with the Department of Computer Science and Information Engineering, Tamkang University, New Taipei City 25137, Taiwan (e-mail: cychang@mail.tku.edu.tw).

Diptendu Sinha Roy is with the Department of Computer Science and Engineering, National Institute of Technology (NIT) Meghalaya, Shillong 793003, India (e-mail: diptendu.sr@nitm.ac.in).

Digital Object Identifier 10.1109/JSEN.2021.3111327

of sensors, achieving high recharging efficiency of the whole sensor networks. However, the newly recharging requests will be sent by sensors which impact the recharging efficiency in terms of the path length and the number of recharged sensors. The predetermined path cannot meet the new recharging requests, which leads to failure of sensors because they are not recharged in time.

Since the disadvantages of the static recharging approaches affect the monitoring performance of the given WSNs, many dynamic recharging mechanisms were proposed recently [14], [18], [19]. In studies [20]–[22], the dynamic recharging mechanisms allowed that sensors with low energy can send their recharging requests to the mobile charger at any time. The mobile charger can timely change the recharging schedule by considering the new requests. Study [21] proposed an offline and online algorithms, aiming to maximize the number of alive sensors while minimizing the total energy consumption for mobile charger. In study [22], the on-demand charging method based on grid partition is used to charging the sensor networks. Since the recharging requests were sent from different sensors at different time slots, the recharging path was update accordingly. The dynamic recharging mechanisms considered the different recharging requirements of each sensor, and adopted effective method to improve the recharging efficiency of the sensors. However, most of them considered the distances between the requested sensors and the mobile charger, aiming to maximize the number of sensors to be recharged.

Different to the existing work, this paper proposes a mobile recharging algorithm, called Coverage Aware Energy Replenish Mechanism (CAERM), which further considers the coverage contribution of each sensor. The mobile charger evaluates the coverage contribution of each requested sensor and selects the sensors with large coverage contribution and short distance as the candidates for energy recharge in the next recharging round. The contributions of this paper are itemized as follows:

A. Considering the Coverage of Each Requested Sensor

Most existing studies [18], [19] considered the distances between the sensors and the mobile charger, aiming to maximize the number of recharged sensors. This paper takes into consideration the coverage of each requested sensor, aiming to maximize the surveillance quality of the monitoring region.

B. Considering the Chain-Effect of the Recharged Sensors

This paper considers not only the coverage contribution and the distance cost of each requested sensor but also the Chain-Effect Recharging Coverage Benefit (CE-RCB). The CE-RCB further considers the cost that a sensor s_i inserted to the path will increase the waiting time and enlarge the sleeping time of the subsequent sensors. This cost is called Chain-Effect, which can reduce the coverage of the later recharged sensors and thus impact the surveillance quality of the WSNs.

C. Dynamic Recharging Schedule

Different from the existing static recharging approaches, this paper dynamically considers the dynamic recharging requests. The Insertion and Deletion conditions are proposed to cooperate the policies of single or multiple updates, aiming to reconstruct the schedule dynamically. Based on the dynamic scheduling, the recharging efficiency can be increased significantly.

The rest of this paper is organized as follows. Section II reviews the related work of recharging mechanisms proposed for WSNs. Section III presents the network environment and problem statement of the investigated issue. Section IV describes the proposed CAERM in detail. Section V gives the simulation experiments and their results. Finally, a conclusion of this paper is drawn in section VI.

II. Related Work

In recent years, the energy problem has become a bottleneck, restricting the applications of wireless sensor networks. In literature, a large number of recharging algorithms based on mobile charger have been proposed to achieve the purpose of sustainable lifetime for a given WSN. These studies can be divided into two classes: static recharging and dynamic recharging. The following reviews these studies and compares them with this work.

A. Static Recharging

In the static recharging algorithms, the mobile charger travels along a fixed path to perform the recharging task for the sensors with insufficient energy. The path is constructed based on the received charging requests from sensors. The recharging schedule will not be changed even if the mobile charger receives new requests from some other sensors. Therefore, how to reduce the distance of the recharging path length is one of the most important issues. Xu *et al.* [14] proposed a partial energy charging model for sensors recharging, aiming to maximize the sensor lifetime and minimize the travel distance of the charger. Since the sensor is partially charged each time, the moving path length of the mobile charger still can be enhanced.

Study [15] proposed a recharging algorithm via partial energy charging, named Heuristic. The proposed algorithm divided the recharging time of a sensor into several time slots. In each recharging tour, the mobile charger performed the recharging task for a sensor several times. A small amount of energy was recharged in each recharging time slot, aiming to shorten the dead durations of sensors. However, the partial energy charging mechanism leads to long recharging path.

In [16], an energy-renewal approach was proposed to ensure the sensor networks working indefinitely. When the residual energy of a sensor was lower than a certain level, a mobile charger is used to recharge it. To optimize the recharging efficiency, the shortest Hamiltonian cycle was constructed to be the optimal traveling path in each renewable cycle. Subsequently, a near-optimal solution was developed to further optimize the recharging path. However, this approach mainly focused on how to construct the recharging path for maximizing the time effectively, the coverage contribution of each sensor was ignored.

To improve the recharging efficiency for the mobile charger, Shu *et al.* [17] studied the velocity control problem of the

mobile charger moving along the charging path. The mobile charger traveled along a pre-planned trajectory. The optimal moving speed of the mobile charger in each sub-path was determined by the given limit recharging waiting time of the next recharged sensor. To achieve the object of maximizing the minimum recharged energy among all nodes in the networks, the sensors with the least "capability of being charged" will not be recharged. Although the recharged capability of the sensor was considered as the criterion to determine the sensor can be recharged in the next cycle, the coverage efficiency and monitoring quality of the network were not considered.

B. Dynamic Recharging

The static recharging scheme was not efficient since the sensors sending new requests might be located near the mobile charger. If the mobile charger can take the new requests into consideration and change its recharging schedule, the path length can be reduced. The dynamic recharging mechanisms further considered the new charging requests from sensors and changed the constructed path accordingly.

He *et al.* [18] proposed a typical dynamic recharging mechanism, called Nearest-Job-Next with Preemption (NJNP). It took both the spatial and temporal properties of the requested sensors into consideration to determine the order of recharging sensors. When the mobile charger completed the recharging task for a sensor, the next to-be-charged sensor selection algorithm was performed again to reselect the next recharging sensor. The requested sensor which was nearest the mobile charger is selected as the recharging target instead of the current recharging target sensor. Since the next recharged sensor was selected according to the distance priority criterion, the sensors far away from the mobile charger might face the starvation problem which leads to death of these sensors, thereby degrading the network lifetime.

Kaswan *et al.* [19] proposed an efficient scheduling scheme for the mobile charger based on gravitational search algorithm (GSA). A Linear Programming (LP) model was first presented for finding an efficient charging schedule for the mobile charger. Then the GSA-based algorithm was performed to determine a recharging scheme for the mobile charger. The primary goal of GSA was expressed by a fitness function which was defined as charging latency. Since the fitness function considered both the temporal and spatial priorities of the requested sensors, the coverage range of requested sensors was not taken into consideration, which made it difficult to maximize the network coverage.

Study [14] proposed a recharging scheme, which aimed to maximize sensor lifetime with the minimal service cost of the mobile charger. It assumed that the sensor can be partially recharged. Firstly, the authors proposed a partial energy charging model for requested sensors to maximize the sum of all the sensor lifetimes. Then it formulated the optimization problems of dispatching a mobile charger to recharge the sensors according to the energy expiration time. However, similar to study [15], the partial energy charging results in long recharging path. In addition, it did not take into consideration the coverage contributions of sensors.

Study [20] proposed a Real-Time On-Demand Charging Scheduling Scheme (RCSS). A prediction model was constructed according to the energy consumption rate which aimed to evaluate the recharging requirement of each sensor. Based on the prediction model, the next recharging sensor selection algorithm was proposed by both considering the dynamic energy consumption of sensors and the distance between the mobile charger and requested sensor. However, different sensors have different coverage contributions. The coverage contributions of sensors were not considered.

Kumar *et al.* [21] proposed an on-demand vehicle-assisted framework for charging, which presented the offline and online algorithms. The offline algorithm divided the monitoring region into several sub-regions. Each sub-region was assigned a WCV to perform the recharging task. In the online algorithm, the requested sensors that the WCV was unable to reach will be removed from the recharging queue. Although the proposed mechanism dynamically adjusted the recharging path, it did not take into consideration the contribution of each sensor. As a result, the surveillance quality still can be improved.

Study [22] proposed an on-demand charging scheme based on grid partition. The monitoring region was divided into several grids. Each grid was assigned with a priority according to the monitoring demand. The mobile charger established the recharging schedule based on the priority of the grid, and firstly recharged the grid with higher priority. However, this scheme causes the situation that the low-priority grids which were closer to the high-priority grids will be placed at the end of the recharging path, resulting in the increase of the constructed path length.

Although the studies in the second category constructed the recharging path in a dynamic manner, none of them considered the coverage contribution of the sensors. Hence, the monitoring quality of the network was unpredictable. Different from the previous studies, this paper proposes a Coverage Aware Energy Replenish Mechanism, named CAERM. The proposed CAERM considers not only the Simple Recharging Coverage Benefit (S-RCB) but also the Chain-Effect Recharging Coverage Benefit (CE-RCB). In addition, the proposed CAERM dynamically considers the dynamic recharging requests. The Insertion and Deletion conditions are proposed to cooperate the policies of single or multiple updates for reconstructing the schedule dynamically. Based on the dynamic scheduling, the recharging efficiency can be increased significantly.

Table I summarizes the comparisons between the proposed mechanism and the related studies in terms of Coverage Contribution, Adjusting Path, Chain-Effect as well as Coverage Efficiency. In comparison, the proposed CAERM takes into consideration the coverage contribution. In addition, the proposed CAERM adjusts the path according to the chain effect and coverage efficiency.

III. Network Environment and Problem Formulation

This section firstly presents the network environment and assumptions of the investigated recharging issue. Then, the problem formulation of this work is described.

TABLE I
COMPARISONS OF PROPOSED *CAERM* AND EXISTING MECHANISMS

Studies	Sensing Contribution	Adjusting Path	Chain-Effect	Coverage Efficiency
[18]	×	×	×	×
[19]	×	×	×	×
[20]	×	○	×	×
[21]	×	○	×	×
[22]	×	○	×	×
[23]	×	○	×	×
[24]	×	○	×	×
Proposed *CAERM*	○	○	○	○

A. Network Environment

This paper considers a monitoring region A. Assume that there are n sensors, $S = \{s_1, s_2, \ldots, s_n\}$, randomly deployed in region A. A base station is deployed in the central location of A, aiming to collect the recharging requests from sensors and forward them to the mobile charger. Each sensor is stationary and powered by a rechargeable battery. Let e_{th}^{charge} and e_{th}^{sleep} denote the predefined *recharging request* and *sleep* thresholds, respectively. Initially, each sensor stays in an active state and performs the sensing task for providing surveillance quality. In the active state, the energy of each sensor is decreased with time. When the remaining energy is smaller than the *recharging request threshold* e_{th}^{charge}, the sensor will send a recharging request to the base station. However, when the remaining energy of sensor is smaller than the *sleep threshold* e_{th}^{sleep}, the sensor will switch to the *sleep* state which can only sleep and wait for the mobile charger to recharge its battery. Since a sensor staying in *sleep* state cannot contribute its coverage, the surveillance quality of region A is decreased with the number of sensors staying in *sleep* state.

Herein, it is noticed that different sensors might send the recharging requests at different time slots. This occurs because that the sensors with different locations have different forwarding loads, which result in different power consumption rates. This also indicates that mobile charger can continuously receive the recharging requests during the execution of the recharging task. The recharging algorithm will be performed round by round. In each round, the mobile charger will perform the following four tasks: (1) checking the current requests maintained in its queue; (2) renewing its recharging schedule by taking into consideration the buffered requests; (3) constructing a new recharging path; (4) moving to the first sensor in its recharging path and recharging the battery of that sensor. Fig. 1 depicts the four tasks performed in each round.

B. Challenges of Recharging Schedule

A mobile charger, denoted by M, which has received the recharging requests of sensors from the base station, aims to schedule the recharging path and perform the recharging task aiming to maximize the surveillance quality of region A. There are two challenges to achieve the goal for the mobile charger M. The first challenge is that the recharging schedule should consider the time cost of movement and the benefit of coverage contribution for the sensors which have already sent the recharging requests. The other challenge is that the recharging schedule should be determined dynamically. That is, the new recharging requests will arrive during the mobile charger performing the recharging task. Recharging the sensors in a requested order might not be the best schedule because that one sensor which sent the request earlier might have a longer distance to the charger.

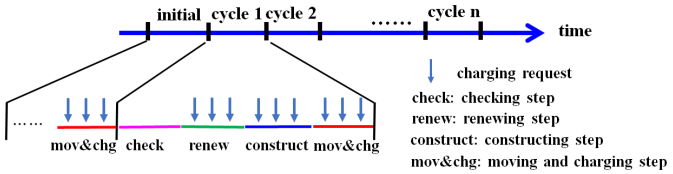

Fig. 1. An example of four tasks performed in each round.

C. Problem Formulation

Coverage is one of the most important indicators to measure the performance of wireless sensor networks. Once sensor s_i switches from *working* to *sleep* states, the coverage of the network will be reduced. This paper proposes a coverage aware recharging algorithm which aims to maximize the network coverage for a given time period T. To achieve this, the coverage contribution of each sensor, which can impact the network coverage, should be taken as an important parameter when developing the recharging algorithm. Consider any sensor s_i. To measure the independent coverage contribution of s_i, the overlapped coverage ranges of s_i and its neighboring sensors should be removed. Let N_i represent the neighbor nodes of s_i. Let notations a_i and a_{N_i} denote the coverage areas of s_i and its neighbor nodes, respectively. The coverage area of a_{N_i} can be represented by Exp. (1).

$$a_{N_i} = \bigcup_{s_j \in N_i} a_j \tag{1}$$

Let $c_{N_i}^t$ denote the coverage contribution of N_i at time t. The value of $c_{N_i}^t$ can be calculated by Exp. (2).

$$c_{N_i}^t = \bigcup_{s_j \in N_i} (a_j * \lambda_j^{work,t}) \tag{2}$$

Then, the independent coverage contribution of s_i at time slot t is expressed as:

$$c_i^t = (a_i - c_{N_i}^t) * \lambda_i^{work,t} \tag{3}$$

The whole coverage contribution, denoted by C^t, of the sensor network can be measured by applying Exp. (4).

$$C^t = \sum_{i=1}^{n} c_i^t \tag{4}$$

Let $T = \{t_1, \ldots t_x\}$ denote the observed time period, which can be partitioned into x time slots. The whole coverage contribution can be represented as:

$$C^T = \sum_{t=t_1}^{t_x} C^t = \sum_{t=t_1}^{t_x} \sum_{i=1}^{n} c_i^t \tag{5}$$

The proposed recharging algorithm aims to maximize the coverage contribution of the given network. Exp. (6) depicts this objective.

1) Objective:

$$Max(C^T) \tag{6}$$

Consider the current round. Let t denote the starting time of the current round. Let $Q = \left\{s_1^Q, s_2^Q, \ldots s_y^Q\right\}$ denote the set of uncompleted requests buffered in request queue. Let $e_i^{rem,t}$ denote the remaining energy at time slot t. Let $\lambda_i^{work,t}$ be a Boolean variable, representing whether or not s_i is in *working* state at time t. That is

$$\lambda_i^{work,t} = \begin{cases} 1 & e_i^{rem,t} > e_{th}^{sleep}(working) \\ . & \\ 0 & e_i^{rem,t} < e_{th}^{sleep}(sleeping) \end{cases} \tag{7}$$

Let $\lambda_i^{request,t}$ denote a Boolean variable, which indicates whether or not s_i has sent a recharging request to M at time slot t. That is

$$\lambda_i^{request,t} = \begin{cases} 1 & e_i^{rem,t} < e_{th}^{charge}(request\ charging) \\ . & \\ 0 & e_i^{rem,t} > e_{th}^{charge}\ (sufficientpower) \end{cases} \tag{8}$$

To better manage the work of each sensor, the following defines three possible states of each sensor and illustrates its major work in each state.

2) Definition: The *working states* of each sensor.

There are three possible *working* states, including *strong working*, *weak working* and *sleep* states. The sensor is said to stay in *strong working* state if the remaining energy is higher than the threshold e_{th}^{charge}. On the other hand, a sensor is said to stay in *weak working* state if its remaining energy is between the recharging request threshold e_{th}^{charge} and the sleep threshold e_{th}^{sleep}. Finally, a sensor is said to stay in *sleep* state if its remaining energy is smaller than sleep threshold e_{th}^{sleep}.

Let $s_i.state$ denote the current state of each sensor, which can only be one of *strong working*, *weak working* and *sleep*. That is,

$$s_i.state = \begin{cases} strong\ working & (\lambda_i^{work,t} = 1, \lambda_i^{request,t} = 0) \\ weak\ working & (\lambda_i^{work,t} = 1, \lambda_i^{request,t} = 1) \\ sleep & (\lambda_i^{work,t} = 0, \lambda_i^{request,t} = 1) \end{cases} \tag{9}$$

Staying in the *strong working* state, each sensor will execute the sensing and data forwarding tasks. However, the two tasks will consume the sensor energy. When the remaining energy of sensor is smaller than the threshold e_{th}^{charge}, it switches to the *weak working* state. In this state, it sends the recharging request to the base station. Then the sensor also performs the sensing and data forwarding tasks. The base station will forward this request to the mobile charger. In case that the remaining energy of the sensor is smaller than the threshold e_{th}^{sleep}, it switches to *sleep* state. The sensor will not perform the sensing and data forwarding tasks if it stays in *sleep* state. This will result in coverage loss.

To illustrate the *working states* of sensor s_i clearly, the following further defines three Boolean variables ρ_i^{SW}, ρ_i^{WW} and ρ_i^{Sleep}, which present the *strong working* state, *weak working* state and *sleep* state, respectively. That is:

$$\rho_i^{SW} = \begin{cases} 1 & if\ s_i.state = Strong\ Workinge \\ . & \\ 0 & otherwise \end{cases} \tag{10}$$

$$\rho_i^{WW} = \begin{cases} 1 & if\ s_i.state = Weak\ Workinge \\ . & \\ 0 & otherwise \end{cases} \tag{11}$$

$$\rho_i^{Sleep} = \begin{cases} 1 & if\ s_i.state = Sleep \\ . & \\ 0 & otherwise \end{cases} \tag{12}$$

For example, when the sensor s_i stays in *strong working* state at time slot t, the values of state parameters are $\rho_i^{SW} = 1, \rho_i^{WW} = 0$ and $\rho_i^{Sleep} = 0$.

Some constraints given blow must be satisfied to achieve the goal of this work. The first constraint is the *state constraint* which restricts any sensor s_i to stay in one of three states at any time slot. Exp. (13) depicts the state constraint.

3) State Constraint:

$$\rho_i^{SW} + \rho_i^{WW} + \rho_i^{Sleep} = 1, \quad \text{for } \forall s_i \in S \tag{13}$$

Another constraint is the recharging request constraint, which indicates that each sensor should send the recharging request to the mobile charger before it entering the sleep state. The following constraint expresses this requirement.

4) Recharging Request Constraint:

$$\lambda_i^{request,t} \geq \lambda_i^{work,t} \quad \text{for } \forall s_i \in S \tag{14}$$

In addition to the *Recharging Request Constraint*, another constraint is *Recharging Efficiency*. Let $d(s_i, s_j)$ represent the distance between sensors s_i and s_j. Assume that the mobile charger visits each sensor along the scheduled path with a constant speed v. Then, the shortest moving time of M from one sensor s_i to the next one s_j can be represented as

$$\frac{\min\limits_{s_i, s_j \in S} d(s_i, s_j)}{v}$$

Let E denote the full battery energy of each sensor. Let notations α^{ch} and α^{disch} denote the recharging rate and discharging rate per unit time, respectively. The following *Recharging Efficiency Constraint* guarantees that the working time of each sensor must be far greater than the sum of the recharging time and the shortest moving time of M.

5) Recharging Efficiency Constraint:

$$\frac{\min\limits_{s_i, s_j \in S} d(s_i, s_j)}{v} + \frac{E}{\alpha^{\mathrm{ch}}} \ll \frac{E}{\alpha^{disch}} \tag{15}$$

IV. The Proposed Algorithm

The movement of mobile charger from the current location to one sensor and recharging the sensor can obtain the benefit of the coverage from the recharged sensor. However, all the other sensors which have sent the recharging requests should wait for longer time because that none of them will be the

next recharged sensor. As a result, some of these sensors might switch from *weak working* state to the *sleep* state, resulting in the disadvantage of coverage loss.

This section presents the recharging algorithms, which aims to construct the recharging path and recharge the sensors which have already sent the recharging requests while satisfying the demand of maximizing the coverage contribution of all sensors. The proposed algorithm, called *CAERM,* dynamically adjusts the recharging path according to the recharging requests of sensors, aiming to minimize the coverage loss for a given WSN. The proposed algorithm will be explained in detail below.

The *CAERM* mainly consists of three phases: the *coverage contribution evaluation* phase, *path construction* phase and *recharging* phase. In the *coverage contribution evaluation* phase, the mobile charger checks the recharging requests queue Q and evaluates the coverage contribution of each sensor in Q. In the *path construction* phase, the mobile charger reviews the schedule determined in the last round by additionally considering the requests in queue, reconstructs the set of candidate sensors and establishes a new recharging path for the candidate sensors. Finally, in the *recharging* phase, the mobile charger moves along the recharging path and charges the next sensor in the path. Since new recharging requests of sensors can be timely sent to the mobile charger, the above mentioned three phases will be executed round by round. The following presents the details of each phase.

A. Coverage Contribution Evaluation Phase

Let P=($s^P_{finished}, s^P_1, s^P_2, \ldots, s^P_{|P|}$) represent the recharging path that has already planned in the last round and the mobile charger has finished the recharging tasks of first sensor $s^P_{finished}$. In case that in the time period of network initialization, the mobile charger can include all the sensors which have sent the requests in queue as the set of recharging candidates and construct an initial path using Hamiltonian path. As a result, the P can be constructed accordingly. Herein, it is noticed that sensors generally have different data forwarding loads and thus their energy consumption rates are different. This can lead to the situation that the recharging requests will be sent from different sensors at different time slots, resulting in a situation that the mobile charger continuously receives recharging requests from different sensors during the execution of the recharging task. Let $R_i = (s_i, (x_i, y_i), t_i)$ denote the recharging request sent by sensor s_i at time t_i, where $l_i = (x_i, y_i)$ denotes the location of sensor s_i. At the time point t, the requested queue maintained by the mobile charger will collect the request R_i from some sensor s_i. Therefore, in each round, the mobile charger should firstly check the current requests in the recharging queue Q after the mobile charger has finished the recharging task for one sensor in the last round. Fig. 2 shows the scenario that the mobile charger checks the recharging requests in current queue Q in the beginning of this round.

To evaluate the coverage contribution of the requested sensors effectively, this phase proposes two algorithms, including *Simple Recharging Coverage Benefit* (*S-RCB)* and *Chain-Effect Recharging Coverage Benefit* (*CE-RCB*) algorithms.

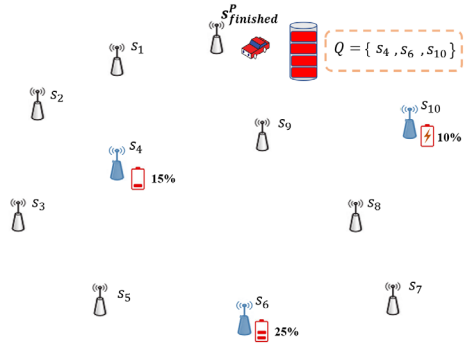

Fig. 2. The scenario that the mobile charger has finished the last round and checks the recharging requests in current queue Q in this round.

The *S-RCB* algorithm aims to calculate the coverage benefit of each requested sensor in queue Q, which is represented by the coverage contribution per movement cost. The *CE-RCB* algorithm further considers *chain effect* which indicates that the recharging of the current sensor can cause the coverage loss of the subsequent recharging sensors. The following presents the details of the proposed two algorithms.

1) Simple Recharging Coverage Benefit (S-RCB) Algorithm:

This subsection illustrates the *S-RCB* algorithm which aims to calculate the recharging benefit of each sensor, and select the sensor with the largest coverage benefit as the next recharging target. Let time t be the current time. Let $Q = \left\{s^Q_1, s^Q_2, \ldots s^Q_y\right\}$ denote the set of sensors which have already sent the recharging requests. Consider any candidate sensor, say s^Q_i, in Q to be selected as the next recharging sensor. Let $\hat{P}$ denote the new recharging path obtained by adding sensor s^Q_i to the recharging schedule. Assuming that sensor s^Q_i is arranged at the *k-th* position in the new recharging path. Then the new recharging path $\hat{P}$ can be represented as $\hat{P} = (s^{\hat{P}}_1, \ldots, s^{\hat{P}}_{k-1}, s^Q_i = s^{\hat{P}}_k, \ldots, s^{\hat{P}}_{|\hat{P}|})$. Let $l_i = (x_i, y_i)$ and $l_j = (x_j, y_j)$ denote the locations of sensors s_i and s_j. Let $d(s_i, s_j)$ denote the distance between sensors s_i and s_j. We have

$$d(s_i, s_j) = ((x_i - x_j)^2 + \left(y_i - y_j\right)^2)^{1/2}$$

Then the coverage benefit of s^Q_i, denoted by B_i, can be calculated by the ratio of increased coverage contribution to the increased recharging path length. Let o^{length}_i denote the overhead of increased path length caused by adding sensor s^Q_i to the recharging path P. The independent coverage contribution c^t_i of s^Q_i at time slot t can be calculated by Exp. (3). The value of B_i can be represented as Exp. (16).

$$B_i = \frac{c^t_i}{o^{length}_i} \tag{16}$$

The *S-RCB* algorithm will simply determine the sensor insertion from queue Q and sensor deletion from path P. To achieve this, two strategies can implement the *S-RCB*: *single update* (*SU*) and *multiple-update* (*MU*) strategies. When considering inserting sensors in Q to path P, the *single-update strategy* inserts at most one sensor from requested queue Q.

Similarly, when considering deleting sensors in path P to Q, the *single-update* strategy also deletes one sensor at most from path P. On the contrary, the *multiple-update strategy* might insert more than one sensors $s_i \in Q$ to the path P. The *multiple-update strategy* also might delete more than one sensors $s_i \in P$ from path P to the queue Q.

The following presents the *single-update strategy*. By applying the single update policy, the *S-RCB* algorithm will calculate the coverage benefit B_i for each sensor $s_i \in Q$ and $s_j \in P$, call B_i^Q and B_j^P, respectively. Let s_{best}^Q and s_{worst}^P denote the sensor with the largest coverage benefit B_i^Q and the sensor with the smallest coverage benefit B_j^P, respectively. That is, we have

$$s_{best}^Q = arg \max_{s_i^Q \in Q} \ B_i^Q$$

$$s_{worst}^P = arg \min_{s_j^P \in P} \ B_j^P$$

Let B_{avg}^Q denote the average coverage benefit of Q. It can be calculated by applying Exp. (17).

$$B_{avg}^Q = (\sum_{i=1}^{|Q|} B_i^Q)/|Q| \tag{17}$$

Similarly, let B_{avg}^P denote the average coverage benefit of P. It can be simply calculated by applying Exp. (18).

$$B_{avg}^P = (\sum_{j=1}^{|P|} B_j^P)/|P| \tag{18}$$

Then B_{avg}^Q can be used as the threshold to determine whether or not sensor s_i^Q should be newly included to the recharging path P. Similarly, and B_{avg}^P can be used as the threshold to determine whether or not sensor s_j^P should be removed from path P. Let B_{best}^Q and B_{worst}^P denote the coverage benefit of sensor s_{best}^Q and s_{worst}^P, respectively. The following presents the *insertion condition* of each sensor $s_i^Q \in Q$ and the *deletion condition* of sensors $s_j^P \in P$.

a) Insertion condition of SU strategy:

$$B_{best}^Q > B_{avg}^P$$

b) Deletion condition of SU strategy:

$$B_{worst}^P < B_{avg}^Q$$

The *Insertion condition* of *SU* strategy mainly implies that sensor s_i^Q in Q can be newly included in path P if it obtains the maximal benefit in Q and the benefit is larger than the average benefit of the nodes which have already in path P. On the other hand, the *Deletion condition* emphases that a node can be removed from path P if it obtains the smallest benefit in P and its benefit is smaller than the average benefit of nodes in Q.

In addition to the *single-update* strategy, the following further presents the *multiple-update* (*MU*) strategy which adds more than one sensors $s_i \in Q$ to path P, and removes more than one sensors $s_i \in P$ from path P to Q. The *insertion condition* and the *deletion condition* of *MU* strategy are given below.

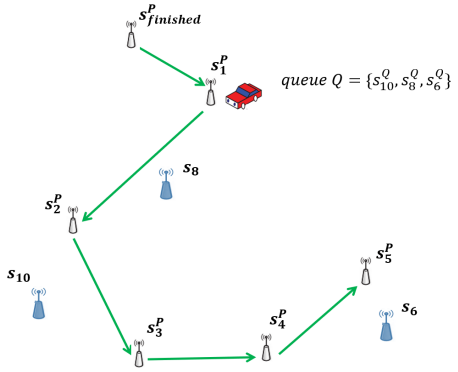

Fig. 3. Coverage contribution evaluation by considering the recharging benefit.

c) Insertion condition of MU strategy:

$$B_i^Q > B_{avg}^P \quad \text{for } s_i \in Q \tag{19}$$

d) Deletion condition of MU strategy:

$$B_j^P < B_{avg}^Q \quad \text{for } s_j \in P \tag{20}$$

The *Insertion condition* of *MU* strategy mainly implies that sensor s_i^Q in Q can be newly included in path P if its benefit is larger than the average benefit of the nodes which have already in path P. On the other hand, the *Deletion condition* emphases that nodes can be removed from path P to Q if their benefits are smaller than the average benefit of nodes in Q.

The following gives an example to illustrate how to apply the insertion and deletion conditions. As shown in Fig. 3, several sensors are deployed in the monitoring region. It is assumed that sensor $s_{finished}$, s_1, s_2, s_3, s_4 and s_5 have been already scheduled in the recharging path P in the last round. That is, we have

$$P = (s_{finished}^P, s_1^P, s_2^P, s_3^P, s_4^P, s_5^P).$$

At the current time t, the mobile charger has finished the recharging task of sensor $s_{finished}$, and has already received the recharging requests sent from sensors s_6, s_8 and s_{10} in the last round. Therefore, we have

$$Q = \{s_1^Q = s_8, s_2^Q = s_{10}, s_3^Q = s_6\}.$$

These sensors in the recharging queue Q are in an order sorted by the receiving time of the recharging request. To determine the best sensor that can be recharged in the next round, the mobile charger evaluates the coverage benefit of each sensor, and then adds the sensor which satisfies the insertion condition to the recharging schedule. The coverage benefits of sensors in Q are calculated as follows.

Applying Exp. (3), the independent coverage contribution of sensor s_8 at time slot t can be expressed as

$$c_8^t = (a_8 - c_{N_8}^t) * \lambda_8^{work,t}$$

where a_8 and $\lambda_8^{work,t}$ represent the coverage range of sensor s_8 and the *working* state of s_8 at time t, respectively. Herein, it is noticed that the value $c_{N_8}^t$ represents the overlap coverage contribution of sensor s_8 and its neighboring sensors.

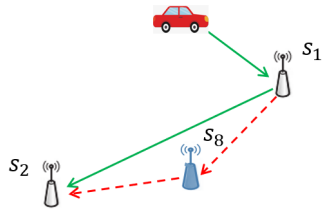

Fig. 4. Coverage benefit of sensor s_8^Q.

Recall that o_8^{length} denotes the overhead of increased path length caused by adding sensor s_8^Q to the recharging path P. As shown in Fig. 4, the value of o_8^{length} can be calculated as shown in Exp. (21).

$$o_8^{length} = d(s_1, s_8) + d(s_8, s_2) - d(s_1, s_2) \tag{21}$$

Therefore, the coverage benefit of sensor s_8^Q can be represented by

$$B_8^Q = \frac{c_8^t}{o_8^{length}}$$

Similarly, the coverage benefits of sensors in queue Q and in path P can be obtained. Finally, the best node s_{best}^Q in Q and the worst node s_{worst}^P in P can be obtained.

$$s_{best}^Q = arg\ \max_{s_i^Q \in Q}\ B_i^Q = s_8^Q$$
$$s_{worst}^P = arg\ \min_{s_j^P \in P}\ B_i^P = s_1^P$$

The average coverage benefits B_{avg}^P and B_{avg}^Q can be calculated accordingly.

$$B_{avg}^P = (\sum_{j=1}^{5}\ B_j^P)/5$$
$$B_{avg}^Q = (\sum_{i=1}^{3}\ B_i^Q)/3$$

Then, one of the proposed two strategies can be applied to determine the sensors which will be recharged in the next round.

(i) Applying the Single Update (SU) Strategy:

For the sensors in Q, the maximal coverage benefit of sensor $s_{best}^Q = s_8^Q$ is compared with the average coverage benefit B_{avg}^P of sensors in P. Sensor s_8^Q will be added in the recharging path if its benefit satisfies the insertion condition $B_8^Q > B_{avg}^P$. On the other hand, the smallest coverage benefit of sensor $s_{worst}^P = s_1^P$ is compared with the average benefit of Q. Sensor s_1^P will be removed from path P to Q if it satisfies the deletion condition $B_1^P < B_{avg}^Q$.

By applying *SU* strategy, the newly recharging sensors in the next round are obtained. Let $\hat{S}$ denote the set of recharging sensors in the next round. We have

$$\hat{S} = \{s_2^P, s_3^P, s_4^P, s_5^P, s_8^Q\}$$

Another policy is to apply the *multiple-update strategy* which might insert more than one sensor $s_i \in Q$ to the path P. It can also remove more than one sensor $s_j \in P$ from path P to Q at a time.

(ii) Applying the Multiple-Update (MU) Strategy:

The main different between SU and MU strategy is the insertion and deletion criteria. The MU strategy should further relax the condition and aim to add more sensors in Q to the path P. Assume that sensors s_8^Q and s_6^Q both satisfy the insertion condition given in Exp. (19), and will be added to the recharging path P. Assume that the coverage benefits of sensors s_1^P and s_5^P are smaller than B_{avg}^Q. As a result, the sensors s_1^P and s_5^P will be removed from path P to Q in the next round. Let $\hat{S}_i^Q$ and $\hat{S}_j^P$ denote the sensors can be included and removed to the recharging path in the next recharging path, respectively. That is

Insertion sensors: $\hat{S}_i^Q = \{s_8^Q, s_6^Q\}$

Deletion sensors: $\hat{S}_j^P = \{s_1^P, s_5^P\}$.

Based on the *multiple-update strategy*, the recharging sensors in the next round have been determined as shown in set $\hat{S}$.

$$\hat{S} = \{s_2^P, s_3^P, s_4^P, s_8^Q, s_6^Q\}.$$

2) Chain-Effect Recharging Coverage Benefit (CE-RCB) Algorithm: The *Chain-Effect Recharging Coverage Benefit*(*CE-RCB*) Algorithm further considers the cost that a sensor s_i inserted to the path will increase the waiting time and enlarge the sleeping time of the subsequent sensors, called *Chain-Effect*, which can reduce the coverage of the later recharged sensors and thus impact the surveillance quality of the WSNs. The following uses the example given in Fig. 2 to illustrate the impact of *chain-effect* on surveillance quality. Assume that the scheduled recharging path is

$$P = (s_{finished}^P, s_1^P, s_2^P, s_3^P, s_4^P, s_5^P).$$

The recharging of sensors s_1^P and s_2^P will increase the waiting time for recharging of sensors s_3^P, s_4^P and s_5^P. The increased waiting time includes the recharging times for sensors s_1^P and s_2^P and the time required for mobile charger to move from s_1^P to s_2^P and from s_2^P to s_3^P. During the waiting period, sensors s_3^P, s_4^P and s_5^P might lose their coverage and switch to the *sleep* state. As a result, the surveillance quality will be reduced. Therefore, *CE-RCB* algorithm determines the sensors to be recharged in the next round by considering the impact of the coverage loss.

Given a scheduled path and a number of recharging requests in queue Q, the *CE-RCB* algorithm aims to examine all sensors in Q and path P and select some of them as the targets of recharging sensors. To achieve this, the coverage benefit of each sensor in Q and P should be evaluated. Herein, we emphasize that a sensor, say s_i, to be recharged will introduce the additional waiting time of subsequent recharging sensors. Let $\Phi(s_i)$ denote the set of subsequent recharging sensors of sensor s_i in the newly constructed path. When the mobile charger moves from the current location to sensor s_i and recharging s_i, each sensor $\in s_j \Phi(s_i)$ will enlarge its waiting time for recharging and hence might be coverage loss. Therefore, the *CE-RCB* algorithm calculates coverage benefit for each sensor $\in s_i P \cup Q$ and the coverage loss of each sensor $\in s_j \Phi(s_i)$. Then the *total coverage benefit* which considers both the increased coverage benefit of sensor s_i and the reduced coverage benefits of $\in s_j \Phi(s_i)$ can be obtained.

The proposed *CE-RCB* algorithm selects the sensors which have higher total coverage benefits to be included in the new path. The following presents the calculation of total coverage benefit of each sensor $\in s_i P \cup Q$. Before that, the waiting time and recharging time of each sensor, which highly depend on recharging and discharging rates, must be calculated firstly.

Assume that mobile charger moves along the recharging path with a constant speed v. Let α^{ch} and α^{disch} denote the recharging and discharging rates, respectively. Let t_i^{wait} denote the waiting time for recharging sensor $\in s_i^P P$. The time t_i^{wait} mainly consists of two parts. The first one is the sum of recharging times of those sensors which are scheduled to be recharged before s_i^P. The second one is the moving time of mobile charger before it arrives to the sensor s_i^P. The waiting time of sensor s_i^P can be expressed as shown in Exp. (22).

Recall that $P = (s^P_{finished}, s_1^P, s_2^P, \ldots, s_{|P|}^P)$ represents the recharging path that has been planned in the last round.

$$t_i^{wait} = \sum_{j=1}^{n-1} t_j^{ch} + \left(\sum_{j=0}^{n-1} d\left(s_j^P, s_{j+1}^P\right)\right)/v \tag{22}$$

Let $e_i^{rem,t}$ denote the remaining energy of sensor s_i^P at time t. Let t_i^{ch} denote the recharging time of sensor s_i^P. We have

$$t_i^{\text{ch}} = (E - e_i^{rem,t} + t_i^{wait} * \alpha^{disch})/\alpha^{ch} \tag{23}$$

To obtain the total coverage benefit of each sensor, the sleeping time of each sensor $\in s_i^P P$ is calculated. Assume that there are totally $m+1$ sensors in the path P. The waiting time t_m^{wait} and recharging time t_m^{ch} of the last sensor s_m^P can be obtained by applying Exps. (22) and (23). Let T denote the total recharging time required for mobile charger to finish a round of recharging task. We have

$$T = t_m^{wait} + t_m^{ch}.$$

Let $t_i^{Max\_working}$ denote the max continuance working time of sensor s_i^P before it switches to the *sleep* state. The $t_i^{Max\_working}$ can be expressed by the remaining energy $e_i^{rem,t}$ and sleeping threshold e_{th}^{sleep} of s_i^P. That is

$$t_i^{Max\_working} = (e_i^{rem,t} - e_{th}^{sleep})/\alpha^{disch} \tag{24}$$

Let T_i^{sleep} denote the sleeping time of sensor s_i^P. We have

$$T_i^{sleep} = [t_1^{sleep}, t_2^{sleep}, \ldots, t_{|T_i^{sleep}|}^{sleep}].$$

In the time period T, the sleeping time of sensor s_i^P can be obtained.

$$T_i^{sleep} = t_i^{wait} - t_i^{Max\_working}$$

Based on the sleeping time of sensor s_i^P, we further define the *working* state of sensor s_i^P at time t. That is

$$\lambda_i^{work,t} = \begin{cases} 0 \quad t \in T_i^{sleep}(sleeping) \\ . \\ 1 \quad otherwise \end{cases} \tag{25}$$

To evaluate the coverage benefit of all sensors $\in s_i P \cup Q$, the *CE-RCB* strategy further analyzes the coverage benefit of these sensors. Let C_P^T denote the obtained coverage benefit of all sensors in path P in the period T. We have

$$C_P^T = \sum_{i=1}^{|P|} \sum_{t=t_1}^{t_x} c_i^t \times \lambda_i^{work,t} \tag{26}$$

Let $C_{\hat{P}}^T$ denote the obtained coverage benefit of the new path $\hat{P}$ which is formed by path P added one more sensor $\in s_i^Q Q$ in the period T. We have

$$C_{\hat{P}}^T = \sum_{i=1}^{|\hat{P}|} \sum_{t=t_1}^{t_x} c_i^t \times \lambda_i^{work,t} \tag{27}$$

Let C_i^T denote the coverage benefit of sensor s_i^Q. It can be derived by applying Exps. (26) and (27).

$$C_i^T = C_{\hat{P}}^T - C_P^T \tag{28}$$

Similarly, the coverage benefit of each sensor $\in s_i P \cup Q$ can be obtained.

Let s_{best}^Q denote the sensor with the largest coverage benefit C_i^T, for all $s_i \in Q$ and let s_{worst}^P denote the sensor with the smallest coverage benefit C_j^T, for all $s_j \in P$. That is, we have

$$s_{best}^Q = arg \max_{s_i \in Q} C_i^T$$
$$s_{worst}^P = arg \min_{s_j \in P} C_j^T$$

Let $C_{avg,Q}^T$ and $C_{avg,P}^T$ represent the average recharging benefits of Q and P, respectively. We have

$$C_{avg,Q}^T = (\sum_{i=1}^{|Q|} C_i^T)/|Q| \quad \text{for } s_i^Q \in Q.$$
$$C_{avg,P}^T = (\sum_{j=1}^{|P|} C_j^T)/|P| \quad \text{for } s_j^P \in P.$$

Then $C_{avg,Q}^T$ and $C_{avg,P}^T$ can be used as the thresholds to determine whether or not sensor s_i^Q should be newly included to the new recharging path, and whether or not sensor s_j^P should be removed from path P. Similar to the *S-RCB* algorithm, the *CE-RCB* algorithm also has two strategies to determine whether or not the sensors $s_i \in Q$ should be newly included in the new path and whether or not the sensor $s_j \in P$ should be removed from path P. The following presents the *single update* (*SU*) and *multiple-update* (*MU*) strategies.

Let C_{best}^Q and C_{worst}^P denote the coverage benefits of sensors s_{best}^Q and s_{worst}^P, respectively. The *Insertion condition* and *deletion condition* of *SU* strategy are presented below.

a) Insertion condition of SU strategy: The sensor $s_{best}^Q \in Q$ should be included in the new path if it satisfies $C_{best}^Q > C_{avg}^P$.

b) Deletion condition of SU strategy: The sensor $s_{worst}^P \in P$ should be removed from path P if it satisfies $C_{worst}^P < C_{avg}^Q$.

Similarly, the *insertion condition* and the *deletion condition* of *MU* strategy are presented.

c) Insertion condition of MU strategy: The sensor $s_{best}^Q \in Q$ should be included in the new path if it satisfies $C_i^Q > C_{avg}^P$, for all $s_i \in Q$.

Determine strategies: The *SU* and *MU* strategies.

Inputs:

1. The sensors having the best and the worst recharging benefits: s^Q_{best}, s^P_{worst};
2. The average recharging benefits B^P_{avg} and B^Q_{avg} in P and Q, respectively ;

Outputs:

$\hat{S}$: the set of recharging sensors in the next round.
Q: the queue of sensors which have sent the recharging requests.

1. ***SU_Insertion Condition***(s^Q_{best}, B^P_{avg})
2. **if** $(s^Q_{best} > B^P_{avg})$
3. $\{ \hat{S} = \hat{S} \cup \{s^Q_{best}\}; \}$
4. **End if**;
5. Return $(\hat{S},Q)$
6. ***SU_Deletion Condition***(s^P_{worst}, B^Q_{avg})
7. **if** $(s^P_{worst} < B^Q_{avg})$
8. $\{ P = P/\{s^P_{worst}\};\ Q = Q \cup s^P_{worst};\ \}$
9. **End if**;
10. Return($\hat{S}$ and Q);
11. ***MU_Insertion Condition***(Q, B^P_{avg})
12. **For each** $s^Q_i \in Q$ **do**
13. **if** $(B^Q_i > B^P_{avg})$
14. $\{ s^Q_i \rightarrow \hat{S};\ \}$
15. **else**
16. $s^Q_i \rightarrow Q$;
17. **End for**
18. Return $(\hat{S}, Q)$
19. ***MU_Deletion Condition***(P, B^Q_{avg})
20. **if** $(s^P_j < B^Q_{avg})$
21. $\{ P \rightarrow s^P_j ;\ s^P_j \rightarrow Q;\ \}$
22. **else**
23. $s^P_{worst} \rightarrow \hat{S}$;
24. Return $\hat{S}$= $\{P\text{-}s^P_j + s^Q_i\}$, Q=$\{P\text{+}s^P_j - s^Q_i\}$;

Fig. 5. Procedure of the *SU* and *MU* strategies.

d) Deletion condition of MU strategy: The sensor $s^P_j \in P$ should be removed from path P if it satisfies $C^P_j < C^Q_{avg}$ for all $s_j \in P$.

The *Coverage Contribution Evaluation Phase* will determine the set of sensors which will be recharged in the next round according to their coverage benefits. Fig. 5 summarizes the proposed *SU* and *MU* strategies in the *Insertion condition* and the *Deletion condition* for the *S-RCB* algorithm.

Figs. 6 and 7 present the proposed *S-RCB* and *CE-RCB* algorithms in the *Coverage Contribution Evaluation Phase*, respectively. As shown in Fig. 6, step 1 calculates the recharging benefit of each sensor in P and Q. Steps 2-7 evaluate the best sensor in Q, the worst sensor in P, and the average recharging benefits of all sensors in path P and queue Q. Steps 8-10 determine the recharged sensors in the next round by applying the *SU* and *MU* strategies. In Fig. 7, steps 2-7 perform two tasks, select the best and worst sensor from Q and P, and calculate the average recharging benefit of all sensors in the *CE-RCB* algorithm. Finally, steps 8-10 detect the sensors recharged in the next recharging round.

B. Path Construction Phase

This phase aims to reconstruct the recharging path according to the set of sensors which satisfy the *Insertion* and *Deletion Conditions*. Herein, we notice that the *Coverage Contribution*

Procedure: ***Simple Recharging Coverage Benefit (S-RCB) Algorithm***

Inputs:

1. A mobile charger M moves with a constant speed v;
2. The recharging request queue Q;
3. The initial location of mobile charger;
4. The recharging parameters: $E, e^{charge}_{th}, e^{sleep}_{th}, \alpha^{ch}, \alpha^{disch}, c^t_{N_i}, o^{length}_i$.

Outputs:

$\hat{S}$ denote the set of recharging sensors in the next recharging round.
Q denote the queue of sensors which have sent recharging request.

/*Calculate the recharging benefit of sensors $s_i \in Q \cup P$ */

1. $B_i = \dfrac{c^t_i}{o^{length}_i}$
2. **For**$(i = 1; i \le |Q|; i++)$ {
3. $s^Q_{best} = arg\max_{s^Q_i \in Q} B^Q_i$
4. $B^Q_{avg} = (\sum_{i=1}^{|Q|} B^Q_i)/|Q|$ }
5. **For**$(j = 1; j \le |P|; j++)$ {
6. $s^P_{worst} = arg\min_{s^P_j \in P} B^P_j$
7. $B^P_{avg} = (\sum_{j=1}^{|P|} B^P_j)/|P|$ }
8. Performing the *Determine strategies;*
9. Return $\hat{S}$=$\{P - s^P_{worst} + s^Q_{best}\}$, $Q = \{P - s^Q_{best} + s^P_{worst}\}$,
10. and $\hat{S}$= $\{P\text{-}s^P_j + s^Q_i\}$, Q=$\{P\text{+}s^P_j - s^Q_i\}$;

Fig. 6. The *S-RCB* algorithm.

Procedure: ***Chain-Effect Recharging Coverage Benefit(CE-RCB) Algorithm***

Inputs:

1. A mobile charger M moves with a constant speed v;
2. The recharging request queue Q;
3. The initial location of mobile charger;
4. The recharging parameters: $E, e^{charge}_{th}, e^{sleep}_{th}, \alpha^{ch}, \alpha^{disch}, c^t_{N_i}, o^{length}_i$.

Outputs:

$\hat{S}$ denote the set of recharging sensors in the next recharging round.
Q denote the queue of sensors which have sent recharging request.

1. Calculate t^{wait}_i and $t^{Max\_working}_i$ according to Exps. (19) and (21)
2. $T^{sleep}_i = T^{sleep}_i - t^{Max\_working}_i$
3. **For**$(i = 1; i \le |Q|; i++)$ {
4. $C^T_i = C^T_{P,i} - C^T_P$;
5. $s^Q_{best} = arg\max_{s_i \in Q} C^T_i$ }
6. **For**$(j = 1; j \le |P|; j++)$ {
7. $C^T_i = C^T_{P\setminus i} - C^T_P$;
8. $s^P_{worst} = arg\min_{s_j \in P} C^T_j$ }
9. Performing the *Determine strategies;*
10. Return $\hat{S}$=$\{P - s^P_{worst} + s^Q_{best}\}$, $Q = \{P - s^Q_{best} + s^P_{worst}\}$,
11. and $\hat{S}$= $\{P\text{-}s^P_j + s^Q_i\}$, Q=$\{P\text{+}s^P_j - s^Q_i\}$;

Fig. 7. The *CE-RCB* algorithm.

Evaluation Phase has determined the set of sensors $\hat{S}^P_j$ which should be removed from path P and the set of sensors $\hat{S}^Q_i$ which should be newly added to the new path. Let the old path P be $P = (s^P_{finished}, s^P_1, s^P_2, \ldots, s^P_{|P|})$. This phase is comprised of two tasks, including the *Removing Task* and *Inserting Task*. The following presents the details of the two tasks.

1) Task1: Removing Task: The goal of this task is to remove the sensors in $\hat{S}^P_j$ from path P. Recall that all sensors in set $\hat{S}^P_j$ satisfy the *Deletion Conditions* and should be removed from

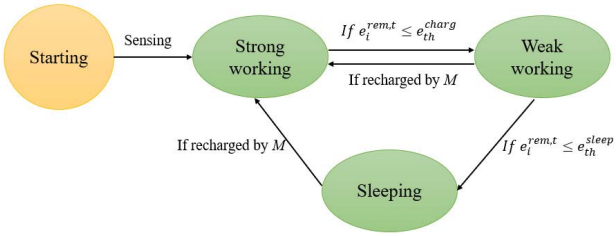

Fig. 8. State transition diagram of each sensor.

path P. Let $P^{sub} = \left(s_{j-1}^P, s_j^P, s_{j+1}^P\right)$ denote the subpath of path P. In this task, the subpath $P^{sub} = \left(s_{j-1}^P, s_j^P, s_{j+1}^P\right)$ will be replaced with the subpath $P^{sub} = \left(s_{j-1}^P, s_{j+1}^P\right)$ for each $s_j^P \in \hat{S}_j^P$.

2) Task2: Inserting Task: This task aims to insert all sensors in set $\hat{S}_i^Q$ to path P, where $\hat{S}_i^Q$ is the set of sensors satisfying the *Inserting Condition* in the previous phase. To obtain a short recharging path, this task first determines the best edge (s_j^P, s_{j+1}^P) in old path P such that it can be replaced with the subpath $(s_j^P, s_i^Q, s_{j+1}^P)$. Let $d\left(s_x, s_y\right)$ denote the distance between two sensors s_x and s_y. Let $l_j^{increse}$ denote the increased length after inserting sensor s_i^Q in edge (s_j^P, s_{j+1}^P). We have

$$l_j^{increse} = d\left(s_j^P, s_i^Q\right) + d\left(s_i^Q, s_{j+1}^P\right) - d\left(s_j^P, s_{j+1}^P\right)$$

Let $(s_{i,j}^{best}, s_{i,j+1}^{best})$ be the best edge for inserting sensor $s_i^Q \in \hat{S}_i^Q$. The best edge should satisfy the following condition.

$$(s_{i,j}^{best}, s_{i,j+1}^{best}) = arg \min_{s_j^P \in P} \; l_j^{increse} \tag{29}$$

The new path $\hat{P}$ can be constructed by adding each sensor $s_i^Q \in \hat{S}_i^Q$ to best edge $\left(s_{i,j}^{best}, s_{i,j+1}^{best}\right)$.

C. Recharging Phase

In this phase, the mobile charger moves along the recharging path $\hat{P}$ with a constant speed and stop at the next sensor in $\hat{P}$ to perform the recharging operation. When the mobile charger finished the recharging task of one sensor, it further checks its request queue Q and performs the Phase A, aiming to determine the new set of recharging sensors and reconstruct its path. The three phases will be repeatedly performed during the lifetime of the WSNs.

Fig. 8 depicts the state transition diagram of each sensor s_i. Initially, each sensor s_i has full energy and stays in a strong working state. Since each sensor consumes energy due to the execution of the monitoring task, it checks whether or not its remaining energy $e_i^{rem,t}$ is smaller than the predefined threshold value e_{th}^{charg}. If it is the case, the sensor will send a recharging request to the base station, record the waiting time as well as switch to the *weak working* state. In this state, the sensor performs the monitoring task and checks whether or not it satisfies the sleep state. If its remaining energy is smaller than the predefined threshold e_{th}^{sleep}, sensor s_i switches to the *sleep* state. In this state, the sensor will not perform the monitoring task. Instead, it will sleep and wait for the mobile charger to recharge the sensor's battery. In case s_i is recharged, it will switch to the *strong working* state.

TABLE II
SIMULATION PARAMETERS

Parameter	value
Monitoring Area	$500m \times 500m$
Number of Sensors	$200 - 400$
Deployment	Random
Discharging rate of sensor	0.05J/s
Battery capacity	3.6kJ
Recharging threshold	320-1520J
Sleep threshold	20-60J
Speed of M	0.5m/s
Recharging Rate	2J /s
Moving consumption Rate	0.01J/s

V. SIMULATION

This section examines the performance improvement of the proposed CAERM against the existing algorithms MERSH [23] and JESRP [24]. The MERSH algorithm [23] planed a charging path in each recharging round by considering the maximum tolerable charging latency and the minimum waiting time of requested sensors. The other compared algorithm, called JESRP [24], which constructed a recharging path based on the important parameters of each sensor, including residual energy of sensors, the future energy consumption rate of sensors, and the charging duration and charging speed of mobile charger. Both of two algorithms focused on wireless recharging for sensors aiming to prolong the lifetime of the networks. The following shows the simulation environment.

A. Simulation Environment

In the experimental study, we use MATLAB 2015 as the simulation tool. A set of rechargeable sensors are randomly deployed over a 500m $\times$ 500m in monitoring area A, as shown in Fig 9. A mobile charger M patrols in the area A aiming to recharge the sensors with insufficient energy. A base station B is deployed at the central location of the monitoring region. It plays the role of static sink which collects data from all sensors in a multi-hop manner. The battery capacity of each sensor is set at 3.6kJ while the energy consumption rate of each sensor is set at 0.05J/s. When the remaining energy of each sensor is lower than the recharging threshold, a recharging request will be sent from that sensor to the base station via multi-hop forwarding. The mobile charger moves with a speed of 0.5m/s, and the recharging rate is 2J/s. The detailed simulation parameters are shown in Table II.

B. Performance Analysis

Fig. 10 compares the coverage of the sensors of three compared algorithms. The coverage is defined by the size of area covered by active sensors divided by the size of the whole monitoring region. As shown in Fig. 10, the coverage of the three compared algorithms are generally decreased with the sleep threshold of sensors. This occurs because that the

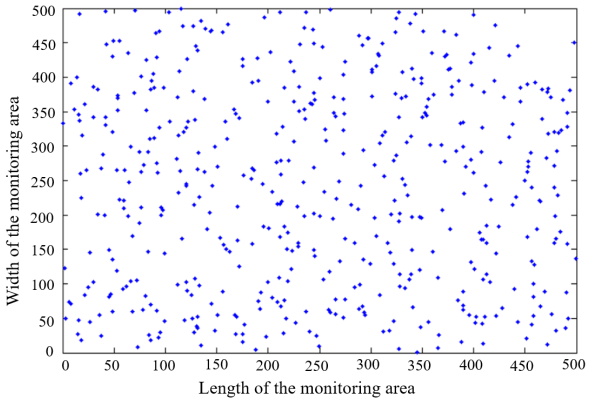

Fig. 9. A screenshot of the considered environment.

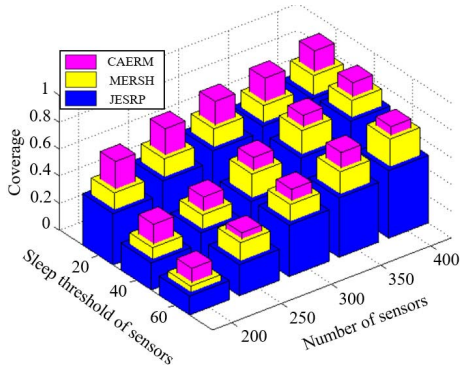

Fig. 10. Performance comparison of CAERM, MERSH and JESRP in terms of coverage by deploying different numbers of sensors and considering different sleep thresholds.

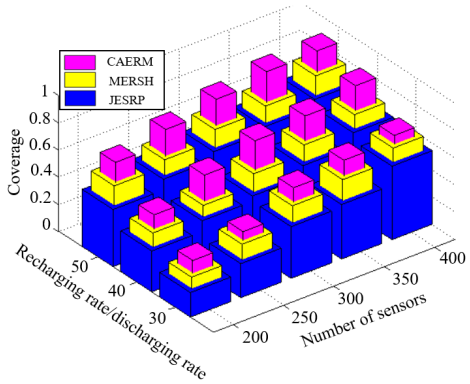

Fig. 11. Performance comparison of CAERM, MERSH and JESRP in terms of coverage by deploying different numbers of sensors and recharging rate/discharging rate.

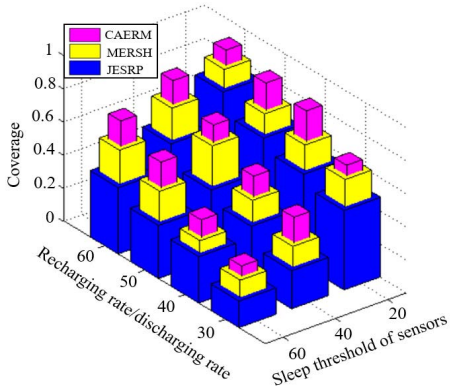

Fig. 12. Performance comparison of CAERM, MERSH and JESRP on coverage with different sleep thresholds and ε values.

smaller sleep threshold leads to longer working time, increasing the coverage. Fig. 10 also reflects the impact of number of sensors on the coverage. A common trend of the compared algorithms is that the coverage is increased with the number of sensors. This occurs because that the increasing number of sensors will enlarge the sensor density. This indicates that the average distance between two sensors has been reduced, which also reduces the movement distance of the mobile charger from one sensor to another. As a result, the mobile charger can charge each sensor with a smaller movement cost. In comparison, the proposed *CAERM* outperforms the other two algorithms in terms of coverage. This occurs because that the proposed *CAERM* constructs the recharging path by considering coverage contribution and moving distance. As a result, the mobile charger usually selects those sensors which have larger coverage contribution and smaller movement cost to be recharged in the next round.

Fig. 11 compares the performance of *CAERM*, *MERSH* and *JESRP* in terms of coverage. The number of sensors varies ranging from 200 to 400. Let ε denote the ratio of recharging rate/discharging rate. That is,

$$\varepsilon = \frac{\alpha^{ch}}{\alpha^{disch}}$$

The value of ε is varied ranging from 30 to 50 percentages. A common trend is that the coverage is increased with the ratio ε in all cases. This occurs because that a large value of ε can reduce the recharging time. As a result, sensors can be recharged as soon as possible and then working for improving the coverage. In comparison, the proposed *CAERM* outperforms the other two compared algorithms. This occurs because that the proposed *CAERM* considers the coverage contribution of each request sensor and the path length of mobile charger when arranging the recharging schedule. However, the two compared *MERSH* and *JESRP* schemes mainly select the fast-consuming sensors, without the consideration of sensor coverage and the path length simultaneously.

Fig. 12 compares the coverage of the three algorithms under different ε value and sleep thresholds. There is a common trend that the coverages of three algorithms increase with the ratio ε, when the sleep threshold is fixed at a certain value. This occurs because that a large value of ratio ε indicates that the sensors can finish recharging task earlier and hence they can work for surveillance. Furthermore, the sleep threshold also affects the coverage. As shown in Fig. 12, a common trend is found that the coverages of all three algorithms are decreased with the sleep threshold. Since the proposed CAERM considers the coverage contribution when selecting the recharging sensors, the proposed algorithm outperforms the other two algorithms in all cases.

Fig. 13 aims to measure the surveillance quality of three algorithms by varying the value of recharging/discharging rates and coverage range. The ratio of energy recharging rate to the energy discharging rate varies ranging from 30 to 60 percentages while the coverage range is varied ranging

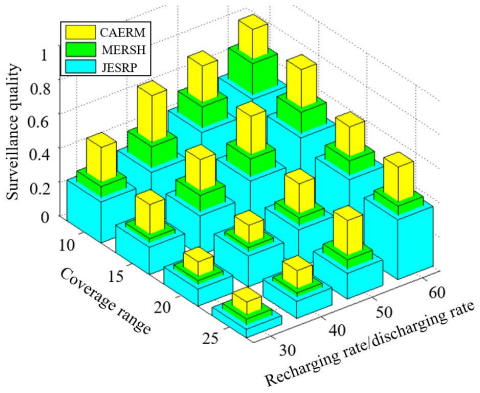

Fig. 13. Comparison of CAERM, MERSH and JESRP in terms of the surveillance quality by varying the coverage range and the recharging/discharging rate.

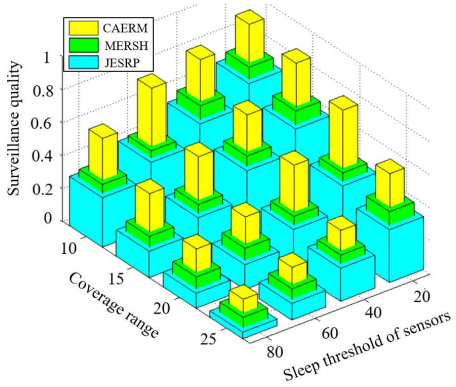

Fig. 14. Comparison of CAERM, MERSH and JESRP in terms of the surveillance quality by varying the coverage range and the sleep threshold of sensors.

from 10 hours to 25 meters. In Fig. 13, a common trend of three algorithms is that the coverage surveillance quality is decreased with the coverage range. This occurs because that the larger coverage range will consume more energy. This leads to a large number of sensors staying in *sleep* state, which results in coverage loss. The energy consumption of each sensor can impact its lifetime and the surveillance quality. A big recharging rate and small discharging rate can improve the remaining energy of each sensor, increasing the network coverage. In comparison, the proposed CAERM outperforms the other two compared algorithms in all cases. This occurs because that the proposed CE-RCB algorithm prior recharges those sensors which contribute larger independent coverage. In addition, the proposed CE-RCB algorithm further considers the chain effect of each sensor. As a result, the proposed CAERM has significant improvement, as compared with the existing MERSH and JESRP.

Fig. 14 further compares the surveillance qualities of three algorithms by varying the coverage range and the sleep thresholds. As shown in Fig. 14, three compared algorithms have a similar trend that their coverages are decreased with the sleep threshold of sensors. This occurs because that the increase of sleep threshold leads to sensor switching its state from *week working* state to *sleep* state earlier, decreasing the network coverage. In comparison, the CAERM outperforms MERSH and JESRP algorithms. This occurs because that the proposed

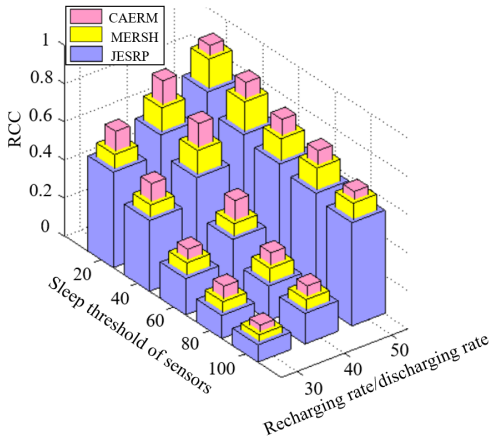

Fig. 15. Comparison of CAERM, MERSH and JESRP in terms of the recharged coverage contribution (*RCC*).

algorithm considers the overall coverage when selecting the recharged sensors.

Fig. 15 compares the Recharged Coverage Contribution (*RCC*) of CAERM, MERSH and JESRP under different sleep threshold of sensors and different recharging/discharging rate. The *RCC* is defined by the total coverage obtained by the recharged sensors divided by the total area of the monitoring region. This measurement aims to evaluate the contribution of the recharged sensors. Let $\varphi_i^{t_i}$ be a Boolean variable which denotes whether or not sensor s_i is recharged at time t_i, $t_i \in T$, where $T = \{t_0, \ldots t_i, \ldots t_x\}$ is a recharging cycle for the mobile charger. Let π_i denote the time length of the *working* state of sensor s_i, including *strong working* and *weak working* states. Once the sensor s_i is recharged at time t_i, the contribution of the recharged sensor can be represented as the total coverage obtained in the future period π_i. The *RCC* can be derived by the following Exp. (30).

$$RCC = \frac{\sum_{i=0}^{i=n} \sum_{t=t_0}^{t_x} (\varphi_i^t \times \sum_{x=t}^{t+\pi_i} c_i^x)}{A} \tag{30}$$

As shown in Fig. 15, a common trend is that the *RCC* values of three compared algorithms significantly increase with ε value. The increase of ε can reduce the recharging time, increasing the number of sensors to be recharged. As a result, the RCC value will be increased. The other common trend is that the RCC value is decreased with the sleep threshold of sensors. When the sleep threshold is increased, the number of sensors switching to *sleep* state will be increased, the RCC value is reduced. In comparison, the proposed CAERM outperforms the existing two compared algorithms. This occurs because the proposed recharging algorithm selects the sensors with the maximal independent coverage contribution to be recharged.

Fig. 16 investigates the Uncharged Coverage Loss (*UCL*) of the three compared algorithms by varying the sleep threshold of sensors and recharging/discharging rate. The uncharged coverage loss is defined by the coverage loss which caused by the requested sensors divided by the total area of the monitoring region. The value of *UCL* can be derived by the

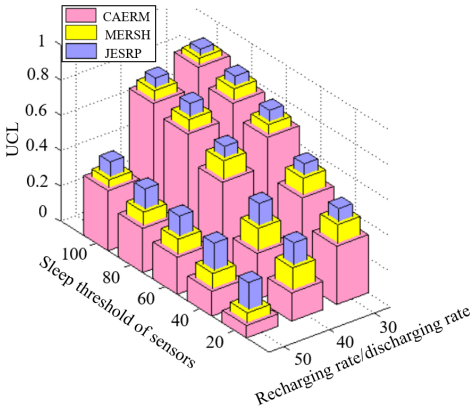

Fig. 16. Comparison of CAERM, MERSH and JESRP in terms of the *Uncharged Coverage Loss* (*UCL*).

following Exp. (31).

$$UCL = \frac{\sum_{i=0}^{i=n} \sum_{t=t_0}^{t=t_x} (c_i^t \times (1 - \lambda_i^{work,t}))}{A} \tag{31}$$

In the experiment, the sleep threshold of the sensors is set ranging from 20 to 100. A common trend can be clearly observed that the *UCL* values of three algorithms increase with the sleep threshold of sensors. This occurs because that the increase of sleep threshold will cause the sensors early to switch to the *sleep* state and therefore result in coverage loss. As a result, the *UCL* value will be increased. Another common trend can be observed that the *UCL* values are decreased with the recharging/discharging ratio. This occurs because that the higher recharging/discharging ratio will reduce the recharging time and hence most recharged sensors can switch to *working* state, reduce the UCL values. In comparison, the proposed CAERM has smaller *UCL* than the other two algorithms. This occurs because that the CAERM prior recharges the sensors with large coverage contribution.

Fig. 17 compares the *Cost Effectiveness Index* (*CEI*) of three recharging algorithms. The number of sensors varies ranging from 200 to 400 while the sleep threshold varies ranging from 20 to 100. The *CEI* is measured by the total obtained coverage divided by the total waiting time of the recharged sensors. Let $\lambda_i^{request}$ be a Boolean variable which denotes whether or not sensor s_i has sent a recharging request in T. The value of *CEI* can be derived by the following Exp. (32).

$$CEI = \frac{\sum_{i=0}^{i=n} \sum_{t=t_0}^{t_x} (\varphi_i^t \times \sum_{x=t}^{t+\pi_i} c_i^x)}{\sum_{i=0}^{i=n} (\lambda_i^{request} \times t_i^{wait})} \tag{32}$$

As shown in Fig. 17, a common trend is that the CEI of three compared algorithms increase with the number of sensors. This occurs because that the increasing number of sensors will reduce average distance between neighboring sensors and hence reduce the moving time of mobile charger along the recharging path. As a result, the coverage obtained from recharged sensors is improved. Another common trend observed from Fig. 17 is that the CEI values of three algorithms are decreased with the sleep threshold. This occurs because that a sensor with higher sleep threshold can cause it

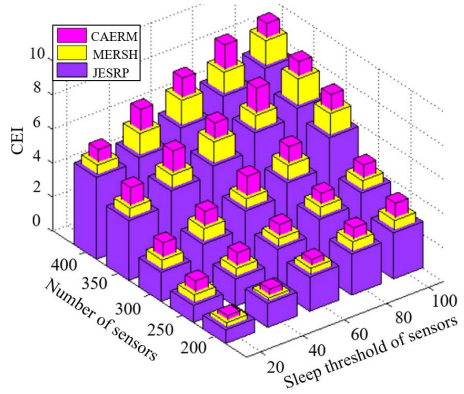

Fig. 17. Performance comparison of CAERM, MERSH and JESRP in terms of coverage of *Cost Effectiveness Index* by varying the sleep thresholds and the number of sensors.

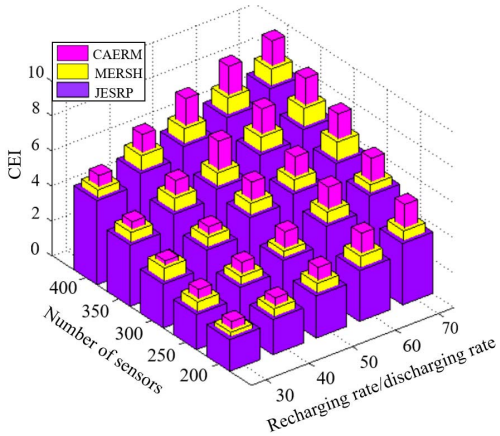

Fig. 18. Performance comparison of CAERM, MERSH and JESRP in terms of coverage of *Cost Effectiveness Index*.

switching to the sleep state earlier, which results in coverage loss. This leads to the reduction of CEI values. In comparison, the proposed CAERM outperforms the other two existing algorithms in all cases. This occurs because that the coverage contribution is considered in the recharging schedule, which aims to maximize the coverage contribution.

Fig.18 compares the *CEI* values of CAERM, MERSH and JESRP by varying the number of sensors and recharging/discharging rate. It is observed that the compared CAERM, MERSH and JESRP algorithms have a similar trend that the *CEI* values are increased with the recharging/discharging rate. This occurs because that the increasing recharging/discharging rate can reduce the time required for recharging. On the other hand, each sensor can stay in longer working time if the discharging rate is smaller. The two reasons can improve the coverage contribution of each recharged sensor and hence enlarge the *CEI* values of three algorithms. In comparison, the proposed CAERM outperforms the other two compared algorithms in terms of the *CEI*. The reasons are presented in what follows. In JESRP, the routing path selection algorithm was adopted to balance the energy of the network. However, the sensor with large coverage contribution was not arranged with a higher priority for recharging. As a result, *CEI* value of JESRP is small. On the other hand, the MERSH constructed the shortest path according to the spatial position of the sensors. However, the coverage contribution of each sensor was

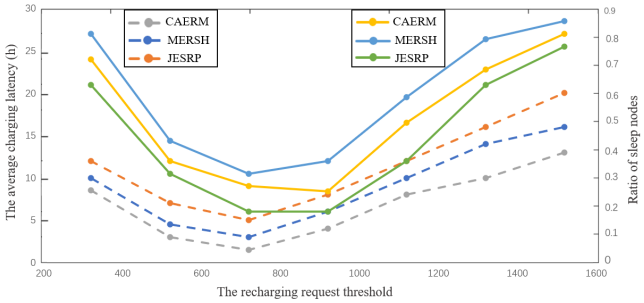

Fig. 19. Performance comparison of CAERM, MERSH and JESRP in terms of the ratio of sleep nodes and the average charging latency.

ignored. Consequently, the coverage contribution of CAERM is larger than those of MERSH and JESRP.

Fig. 19 compares the three algorithms in terms of the ratio of sleep nodes and the average charging latency. The recharging request threshold of each sensor is varied ranging from 320 to 1520J. As shown in Fig. 19, the three compared algorithms have a similar trend that the ratio of sleep nodes is firstly decreased and then increased with the recharging request threshold. The increasing recharging request threshold can help sensors obtain more recharging opportunities since the mobile charger receives the recharging request earlier and thus arrives at the requested sensor before it suffering energy shortage. However, when the threshold value is larger than 720J, the mobile charger arrives at the requested sensor too early. This cause the requested sensor still has rich energy and hence the recharging efficiency of mobile charger is low. Therefore, the request sensors which have small coverage contribution lose the recharge opportunities due to the low recharging efficiency of mobile charger. As a result, the ratio of sleep nodes is increased. In comparison, the three compared algorithms have similar performance results since they have the common goal to recharge as more as possible sensors which have low energy. This also leads to the curves of average charging latency and the ratio of sleep nodes are similar. In comparison, the three algorithms have similar performance because that they all concern the recharging request threshold and propose policies to reduce the number of sleep nodes. Though the proposed CAERM has a similar performance as compared with the other two algorithms, it outperforms the other two algorithms in terms of ~~the~~ surveillance quality (coverage). This occurs because that the goal of the proposed CAERM takes into consideration the coverage contribution of the sensors.

VI. Conclusion

This paper proposes a mobile recharging algorithm, called *CAERM*, which aims to recharge the sensors deployed in a given monitoring area. The proposed *CAERM* considers the coverage of each request sensor while constructing the recharging path, aiming to maximize the surveillance quality of the given networks. The proposed *CAERM* consists of three phases: *Coverage Contribution Evaluation*, *Path construction* and *Recharging phases*.

The first phase aims to select the sensors to be recharged in the next round by calculating the coverage contribution of each requested sensor. Herein, two algorithms are proposed to evaluate the coverage contribution of each sensor, including the *S-RCB* and *CE-RCB*. The *S-RCB* algorithm aims to calculate the recharging benefit of each sensor. On the other hand, the *CE-RCB* algorithm further considers the cost that a sensor s_i inserted to the path will increase the waiting time and enlarge the sleeping time of the subsequent sensors. In addition to the calculation of coverage contribution, two sensors update strategies, including *single update (SU)* and *multiple-update (MU)*, are used to determine the recharging sensors in the next round.

The second phase, called *Path Construction Phase*, further planes the recharging schedule of the selected sensors according to the shortest path construction method. Finally, in the *Recharging Phase*, the mobile charger performs the recharging task of the first scheduled sensor along the recharging path constructed in the second phase. Experimental studies show that the proposed *CAMERM* outperforms existing schemes in terms of coverage, coverage contribution, uncharged coverage loss as well as cost effectiveness index.

References

[1] M. T. Lazarescu and P. Poolad, "Asynchronous resilient wireless sensor network for train integrity monitoring," *IEEE Internet Things J.*, vol. 8, no. 5, pp. 3939–3954, Mar. 2021.

[2] L. Xie, Y. Shi, Y. T. Hou, and A. Lou, "Wireless power transfer and applications to sensor networks," *IEEE Wireless Commun.*, vol. 20, no. 4, pp. 140–145, Aug. 2013.

[3] T. M. Behera, S. K. Mohapatra, U. C. Samal, M. S. Khan, M. Daneshmand, and A. H. Gandomi, "Residual energy-based cluster-head selection in WSNs for IoT application," *IEEE Internet Things J.*, vol. 6, no. 3, pp. 5132–5239, Jun. 2019.

[4] G. Koppala and R. L. Velusamy, "Prototype of home monitoring device using Internet of Things and river formation dynamics-based multi-hop routing protocol (RFDHM)," *IEEE Trans. Consum. Electron.*, vol. 65, no. 3, pp. 329–338, Aug. 2019.

[5] P. Chanak and I. Banerjee, "Congestion free routing mechanism for IoT-enabled wireless sensor networks for smart healthcare applications," *IEEE Trans. Consum. Electron.*, vol. 66, no. 3, pp. 223–232, Aug. 2020.

[6] W. Lu *et al.*, "Energy efficiency optimization in SWIPT enabled WSNs for smart agriculture," *IEEE Trans. Ind. Informat.*, vol. 17, no. 6, pp. 4335–4344, Jun. 2021.

[7] G. S. Dhunna and I. Al-Anbagi, "A low power WSNs attack detection and isolation mechanism for critical smart grid applications," *IEEE Sensors J.*, vol. 19, no. 13, pp. 5315–5324, Jul. 2019.

[8] G. Han, X. Yang, L. Liu, and W. Zhang, "A joint energy replenishment and data collection algorithm in wireless rechargeable sensor networks," *IEEE Internet J.*, vol. 5, no. 4, pp. 2596–2604, Aug. 2018.

[9] C.-Y. Chang, S.-Y. Chen, I.-H. Chang, G.-J. Yu, and D. S. Roy, "Multi-rate data collection using mobile sink in wireless sensor networks," *IEEE Sensors J.*, vol. 20, no. 14, pp. 8173–8185, Jul. 2020.

[10] K. Liu *et al.*, "An active mobile charging and data collection scheme for clustered sensor networks," *IEEE Trans. Veh. Technol.*, vol. 68, no. 5, pp. 5100–5113, Mar. 2019.

[11] M. Angurala, M. Bala, and S. S. Bamber, "Performance analysis of modified AODV routing protocol with lifetime extension of wireless sensor networks," *IEEE Access*, vol. 8, pp. 10606–10613, Jan. 2020.

[12] C. Lin, J. Zhou, C. Guo, H. Song, G. Wu, and M. S. Obaidat, "TSCA: A temporal-spatial real-time charging scheduling algorithm for on-demand architecture in wireless rechargeable sensor networks," *IEEE Trans. Mobile Comput.*, vol. 17, no. 1, pp. 211–224, Jan. 2018.

[13] Y. Feng, N. Liu, F. Wang, Q. Qian, and X. Li, "Starvation avoidance mobile energy replenishment for wireless rechargeable sensor networks," in *Proc. IEEE ICC*, Kuala Lumpur, Malaysia, May 2016, pp. 1–6.

[14] W. Xu, W. Liang, X. Jia, Z. Xu, Z. Li, and Y. Liu, "Maximizing sensor lifetime with the minimal service cost of a mobile charger in wireless sensor networks," *IEEE Trans. Mobile Comput.*, vol. 17, no. 11, pp. 2564–2577, Nov. 2018.

[15] W. Xu, W. Liang, X. Jia, and Z. Xu, "Maximizing sensor lifetime in a rechargeable sensor network via partial energy charging on sensors," in *Proc. IEEE SECON*, London, U.K., Jun. 2016, pp. 1–6.
[16] L. Xie, Y. Shi, Y. Hou, and H. D. Sherali, "Making sensor networks immortal: An energy-renewal approach with wireless power transfer," *IEEE/ACM Trans. Netw.*, vol. 20, no. 6, pp. 1748–1761, Dec. 2012.
[17] Y. Shu *et al.*, "Near-optimal velocity control for mobile charging in wireless rechargeable sensor networks," *IEEE Trans. Mobile Comput.*, vol. 15, no. 7, pp. 1699–1713, Jul. 2016.
[18] A. Kaswan, A. Tomar, and P. K. Jana, "An efficient scheduling scheme for mobile charger in on-demand wireless rechargeable sensor networks," *J. Netw. Comput. Appl.*, vol. 114, no. 15, pp. 123–134, Jul. 2018.
[19] L. He, Y. Gu, J. Pan, and T. Zhu, "On-demand charging in wireless sensor networks: Theories and applications," in *Proc. IEEE 10th Int. Conf. Mobile Ad-Hoc Sensor Syst.*, Hangzhou, China, Oct. 2013, pp. 28–36.
[20] P. Zhong, Y. Zhang, S. Ma, X. Kui, and J. Gao, "RCSS: A real-time on-demand charging scheduling scheme for wireless rechargeable sensor networks," *IEEE Sensors*, vol. 18, no. 5, p. 1601, May 2018.
[21] R. Kumar and J. C. Mukherjee, "On-demand vehicle-assisted charging in wireless rechargeable sensor networks," *Ad Hoc Netw.*, vol. 112, no. 1, Mar. 2021, Art. no. 102389.
[22] Q. Hu, J. Yang, Y. Huo, B. Li, and S. Li, "Space-correlation-based joint data transmission and on-demand charging for rechargeable wireless sensor networks," *IET Commun.*, vol. 15, no. 4, pp. 546–557, Dec. 2020.
[23] Y. Feng, L. Guo, X. Fu, and N. Liu, "Efficient mobile energy replenishment scheme based on hybrid mode for wireless rechargeable sensor networks," *IEEE Sensors J.*, vol. 19, no. 21, pp. 10131–10143, Nov. 2019.
[24] L. Tang, J. Cai, J. Yan, and Z. Zhou, "Joint energy supply and routing path selection for rechargeable wireless sensor networks," *IEEE Sensors*, vol. 18, no. 6, p. 1962, Jun. 2018.

Hongli Yu received the bachelor's degree from Inner Mongolia Teaching University, China, in 2009, and the master's degree from Nanhua University in 2013. From 2013 to 2019, she was a Teacher with Chuzhou University, Anhui, China. Since 2020, she has been a Teacher with Liaoning University of Technology, Jinzhou, China. Her current research interests include wireless sensor networks, the Internet of Things, health care, and wireless localization.

Chih-Yung Chang (Member, IEEE) received the Ph.D. degree in computer science and information engineering from National Central University, Taiwan, in 1995. He is currently a Distinguish Professor with the Department of Computer Science and Information Engineering, Tamkang University, New Taipei City, Taiwan. His current research interests include artificial intelligence, the Internet of Things, wireless sensor networks, and smart healthcare. He has served as an Associate Guest Editor for several SCI-indexed journals, including *International Journal of Ad Hoc and Ubiquitous Computing* (IJAHUC) from 2011 to 2021, *International Journal of Distributed Sensor Networks* (IJDSN) from 2012 to 2014, *IET Communications* in 2011, *Telecommunication Systems* (TS) in 2010, *Journal of Information Science and Engineering* (JISE) in 2008, and *Journal of Internet Technology* (JIT) from 2004 to 2008.

Yajun Wang received the B.S. and M.S. degrees in electronics information engineering from Shenyang Normal University, Shenyang, China, in 2001 and 2004, respectively, and the Ph.D. degree in control theory and control engineering from Northeastern University, Shenyang, in 2015. From 2004 to 2014, she was a Teacher with Liaoning University of Technology, Jinzhou, China, where she has been a Professor since 2020. She has authored more than 30 articles. Her research interests include multivariate statistical modeling, process monitoring, and fault diagnosis and their applications in industry process.

Diptendu Sinha Roy received the Ph.D. degree in engineering from Birla Institute of Technology, Mesra, India, in 2010. In 2016, he joined the Department of Computer Science and Engineering, National Institute of Technology (NIT) Meghalaya, India, as an Associate Professor, where he has been serving as the Chair of the Department of Computer Science and Engineering since January 2017. Prior to his stint at NIT Meghalaya, he was with the Department of Computer Science and Engineering, National Institute of Science and Technology, Brahmapur, India. His current research interests include software reliability, distributed and cloud computing, and the IoT, specifically applications of artificial intelligence/machine learning for smart integrated systems. Dr. Sinha Roy is a member of the IEEE Computer Society.

Xing Bai is currently pursuing the bachelor's degree with Liaoning University of Technology, Jinzhou, China. Her research interests include the Internet of Things and wireless sensor networks.